

Weighing the young stellar discs around Sgr A*

Sergei Nayakshin^{1,2}, Walter Dehnen¹, Jorge Cuadra² & Reinhard Genzel^{3,4}

¹Department of Physics & Astronomy, University of Leicester, Leicester, LE1 7RH, UK

²Max-Planck-Institut für Astrophysik, Karl-Schwarzschild-Straße 1, 85741 Garching bei München, Germany

³Max-Planck-Institut für Extraterrestrische Physik (MPE), Garching bei München, Germany

⁴Department of Physics, University of California, Berkeley, CA 94720, USA

24 August 2018

ABSTRACT

It is believed that young massive stars orbiting Sgr A* in two stellar discs on scales of $\sim 0.1 - 0.2$ parsecs were formed either farther out in the Galaxy and then quickly migrated inward, or in situ in a massive self-gravitating disc. Comparing N-body evolution of stellar orbits with observational constraints, we set upper limits on the masses of the two stellar systems. These masses turn out to be few times lower than the expected total stellar mass estimated from the observed young high-mass stellar population and the standard galactic IMF. If these stars were formed in situ, in a massive self-gravitating disc, our results suggest that the formation of low-mass stars was suppressed by a factor of at least a few, requiring a top-heavy initial mass function (IMF) for stars formed near Sgr A*.

Key words: Galaxy: centre – accretion: accretion discs – galaxies: active – stars: formation

1 INTRODUCTION

Sgr A* is a $M_{\text{BH}} \sim 3.5 \times 10^6 M_{\odot}$ super-massive black hole (SMBH) in the centre of our Galaxy (e.g., Schödel et al., 2002; Ghez et al., 2003). Few tens of close young massive stars dominate the energy output of the central parsec of the Galaxy (Krabbe et al., 1995; Genzel et al., 2003). The ages of the young stars are estimated at $t = 6 \pm 1$ million years (Paumard et al., 2005). The origin of these stars is an important mystery for astrophysics of Active Galactic Nuclei (AGN). “Normal” modes of star formation at 0.1 pc distances from a SMBH are forbidden due to the huge tidal field of the central object. Star formation in a massive gravitationally unstable accretion disc (Paczyński, 1978; Kolykhalov & Sunyaev, 1980; Collin & Zahn, 1999; Goodman, 2003) has been suggested (Levin & Beloborodov, 2003; Milosavljević & Loeb, 2004; Nayakshin & Cuadra, 2005). Alternatively, the observed close young stars could be remnants of a massive young star cluster whose orbit decayed due to dynamical friction (e.g., Gerhard, 2001; Kim & Morris, 2003; Kim et al., 2004; McMillan & Portegies Zwart, 2003; Gürkan & Rasio, 2005).

A successful model for the origin of young stars in Sgr A* will have to explain quantitatively not only the creation of the stars but also their present day orbits. Almost all of the observed young stars in Sgr A* belong to one of two *stellar* rings (Levin & Beloborodov, 2003; Genzel et al., 2003). Internal N-body disc evolution sets an upper limit on the total mass of each of the stellar systems of the order of

$M \lesssim 3 \times 10^5 M_{\odot}$, too high to be constraining for either of the models (Nayakshin & Cuadra, 2005). In addition to the internal disc thickening, discs precess in their mutual (non axi-symmetric) potential and are warped with time (Nayakshin, 2005). Stellar discs that end up too strongly warped or thick will contradict the observations. Nayakshin & Cuadra (2005) suggested that this sets an upper limit on the total stellar mass in the range of $M \lesssim (3 - 10) \times 10^4 M_{\odot}$, but noted that more detailed tests are needed.

The goal of this paper is to perform such tests numerically. Let us estimate the magnitude of the warping effect. Nayakshin (2005) calculated the rate at which a massless accretion disc is warped by a massive ring inclined with respect to the (initially flat) disc at an angle β . For radii R much smaller or much larger than the ring radius, R_{ring} , the precession angular frequency $\omega_p(R)$ can be approximated as

$$\frac{\omega_p(R)}{\Omega_K(R)} \approx -\frac{3M_{\text{ring}}}{4M_{\text{BH}}} \cos \beta \frac{R^3 R_{\text{ring}}^2}{[R^2 + R_{\text{ring}}^2]^{5/2}}. \quad (1)$$

Here M_{ring} is the ring mass, assumed to be much smaller than the blackhole mass, M_{BH} , and $\Omega_K(R)$ is the Kepler circular frequency for the disc at radius R . The period of circular motion $3''$ ($1'' \approx 0.04$ pc at the distance of Sgr A*) away from Sgr A*, where most of the bright young stars are found, is around 2 thousand years. Therefore, the stars at this location make about a thousand revolutions in a few million years. Let $\Delta\gamma = \omega_p t$ be the angle on which an annulus of the disc will precess during this time: $\Delta\gamma \sim (M_{\text{ring}}/M_{\text{BH}}) \times 1000$.

Very approximately, the disc warping will be noticeable when $\Delta\gamma \sim 1$. Thus mass ratios ($M_{\text{ring}}/M_{\text{BH}}$) in excess of 10^{-3} or so may lead to warping of the stellar discs in Sgr A*.

Equation 1 depends on the angle β , and would also depend on the eccentricity of a stellar orbit if it were not assumed to be zero in the derivation. Stars are expected to be born on nearly circular Keplerian orbits (e.g., Nayakshin & Cuadra, 2005), i.e. with eccentricity $e \sim H/R \ll 1$, for star formation in a self-gravitating disc. On the other hand, Levin et al. (2005) have recently demonstrated that, due to a repetitive interaction with the IMBH, stars peeled off the IMBH-star cluster gain a substantial eccentricity to their orbits. Even for the case of the circular IMBH inspiral, stars acquire a mean eccentricity of $e \approx 0.5$. We may thus expect different mass limits for the two models of the origin of the young stars near Sgr A*.

Reader not interested in the technical details of the simulations and data comparison may simply look up the relevant limits and proceed to the discussion of the results in §5.

2 NUMERICAL METHOD

To follow stellar orbits, we use the N-body package ‘NEMO’ (Teuben, 1995) with the orbit integrator ‘gyrfalcon’ (Dehnen, 2002). The code calculates gravitational interaction of all the particles and updates their velocities and positions. We model the blackhole as a Plummer sphere with a core radius of $0.01''$. This radius is much smaller than peri-centres of stellar orbits we consider. The stars are represented as particles with softening radius of $0.01''$ or less for some tests. Depending on the total mass of the stars, we use between few hundred to few thousand particles for each of the two stellar systems.

To set up the problem, we shall rely on the gross results of Genzel et al. (2003), and the more recent analysis of the data by Paumard et al. (2005). For convenience only, we shall refer to the clock-wise rotating system in the GC as a disc, and the counter clock-wise system as a ring. To model the disc, we start with stars in a flat disc with the radial extent from $R_{\text{in}} = 2''$ to $R_{\text{out}} = 5''$. The observed counter clock-wise system contains fewer stars and it is harder to assign the radial extent for this system (Paumard et al., 2005). We used two plausible guesses for the ring, therefore: one is a ring between $R_{\text{in}} = 4''$ and $R_{\text{out}} = 5''$, and the other is a ring between $R_{\text{in}} = 5''$ and $R_{\text{out}} = 7''$. The initial inclination between the two systems is set at $\beta = 113^\circ$ (Genzel et al., 2003; Paumard et al., 2005). Other parameters of initial conditions specific to a model will be discussed below.

The simulations were ran until time $t \approx 3$ Million years. To ensure numerical precision, the individual timesteps of the particles were kept small enough, e.g. in the range of 0.06 to 2 years. The angular momentum and total energy of the system were conserved to a relative error of 10^{-3} or better. We did not include the isotropic cluster of late type stars around Sgr A* in these simulations because in the radial range of interest its mass is small compared to that of Sgr A*, and it would not present any torques for the discs because of the cluster’s spherical symmetry.

At the end of a simulation, we fit the two stellar systems by a plane in velocity space, (v_x, v_y, v_z) . A plane is charac-

terised by vector \vec{n} orthogonal to the plane and normalised to unity, $\vec{n}^2 = 1$. The best fitting planes are found via the reduced χ^2 method for both of the two stellar systems. The reduced χ^2 for a fit is defined as in Levin & Beloborodov (2003):

$$\chi^2 = \frac{1}{N_s - 1} \sum_{i=1}^{N_s} \frac{(v_x n_x + v_y n_y + v_z n_z)^2}{(\sigma_x n_x)^2 + (\sigma_y n_y)^2 + (\sigma_z n_z)^2}, \quad (2)$$

where N_s is the number of stars in the given stellar system, n_x, n_y and n_z are the projections of \vec{n} , and σ_x, σ_y and σ_z are the errors in stellar velocities in the three directions. For simplicity we assume that these errors are isotropic, i.e. each component is equal to $\sigma/\sqrt{3} \approx 40$ km/sec, where $\sigma = 70$ km/sec, the typical value for the absolute value of velocity error vector in Paumard et al. (2005).

Finally, to emulate the effects that the observational errors have on the χ^2 fits through statistical scatter of the data around the mean, we added random Gaussian velocity kicks to each star’s velocity vectors according to the errors σ_x , etc, at the end of the simulations.

3 EXAMPLE RUNS FOR CIRCULAR INITIAL STELLAR ORBITS

As explained in §2, we start with the two stellar systems oriented as the observed best fitting planes (Paumard et al., 2005). The discs are populated by star particles with surface density $\Sigma(R) \propto R^{-2}$ for $R_{\text{in}} \leq R \leq R_{\text{out}}$. The initial velocity dispersion of stars with respect to the local circular Kepler velocity is isotropic and small, $\langle |\vec{v} - \vec{v}_K| \rangle = 0.017v_K$, consistent with the small initial gaseous disc thickness.

A convenient way to illustrate the results is via the ‘Aitoff map projection’ of the stellar orbits. Each stellar orbital plane can be characterised by the inclination angle i with respect to the observer and the position angle ϕ which reflects the position of the lines of the nodes of the orbit on the plane of the sky (e.g. Schödel et al., 2002; Ghez et al., 2003; Eisenhauer et al., 2005; Ghez et al., 2005). The normal vectors to the plane, introduced above, are related to these angles as $n_z = \cos i$, $n_x = \sin i \cos \phi$, and $n_y = \sin i \sin \phi$. The Aitoff’s projection then shows the latitude, defined as $\pi/2 - i$, and longitude = ϕ .

Figure 1 shows the state of the two stellar systems 3 million years into one of the simulations, e.g. the final state. The total stellar masses in the disc and the ring systems (CW and CC systems, respectively) used in this simulation are noted in the left upper corner of the Figure. The stars in the clock-wise system (marked as CW on the Figure) are shown with green asterisks, whereas the counter-clockwise system is shown with red crosses, marked as CC. The lower left corner shows the resulting values of the minimum reduced χ^2 values as a (ring, disc) pair. These are comfortably smaller than the observed values $\chi_{\text{cw}}^2 = 2.5$ and $\chi_{\text{cc}}^2 = 4.0$ for the clock-wise and the counter clock-wise stellar systems, respectively (Paumard et al., 2005). Apparently such a weak disc warping would not contradict observations.

Figure (2), shows the same numerical experiment but with the disc and ring masses both around $10^4 M_\odot$. As is clear from the Figure, both systems suffer considerably from the gravitational torques imposed on each other, and the

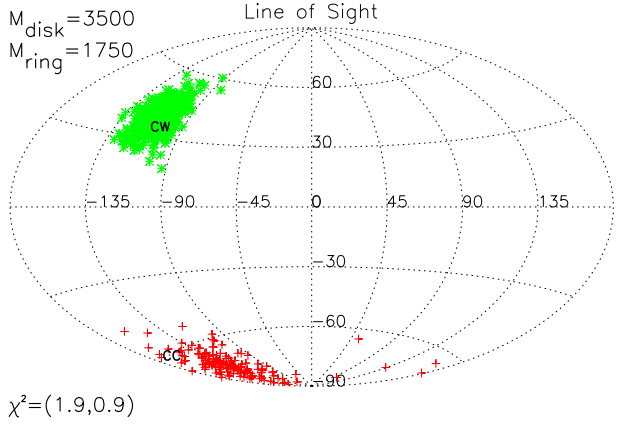


Figure 1. The orientation angles of the stellar orbital planes, as described in the text. The positions of the clockwise and counter-clockwise systems are shown with symbols CW and CC, respectively. Total disc and ring masses are labelled at the upper left corner. The values of the minimum reduced χ^2 fits to the (ring, disc) systems are displayed in the lower left corner of the Figure.

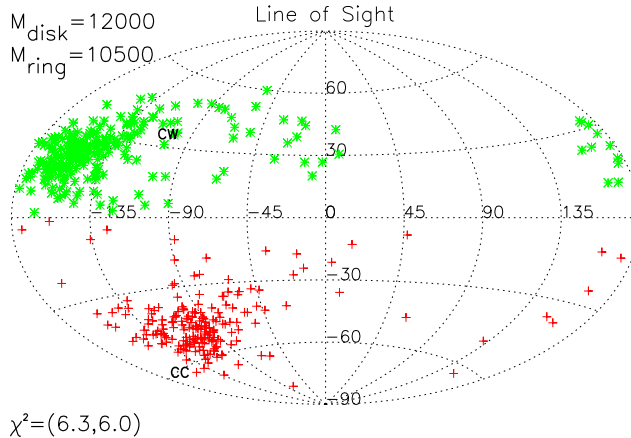


Figure 2. Same as Figure 1 but for much higher disc and ring masses. Note that this stellar distribution is somewhat inconsistent with the data, with the reduced χ^2 values exceeding the observed values of $\chi^2_{cc,cw} = (4.0, 2.5)$.

resulting plane-parallel fits to these are poorer than before. The reduced χ^2 values are larger than the observed values for both the clock-wise and the counter clock-wise systems.

Figure 3 presents the Aitoff map for the most massive case that we have explored, with the disc and ring masses both around $3.5 \times 10^4 M_\odot$. The resulting χ^2 values are quite large and are clearly inconsistent with the data. Note that the degree of mixing occurring in this simulation is extreme, and some of the particles that originally belonged to the clock-wise disc are now classified as members of the counter-clockwise system. A stellar system with such poor values of χ^2 may not even remotely be considered as consisting of two or one stellar discs, obviously.

In this latest example we have seen that stars from one system may evolve on orbits more consistent with the other system, and it would then be improper to continue to assign

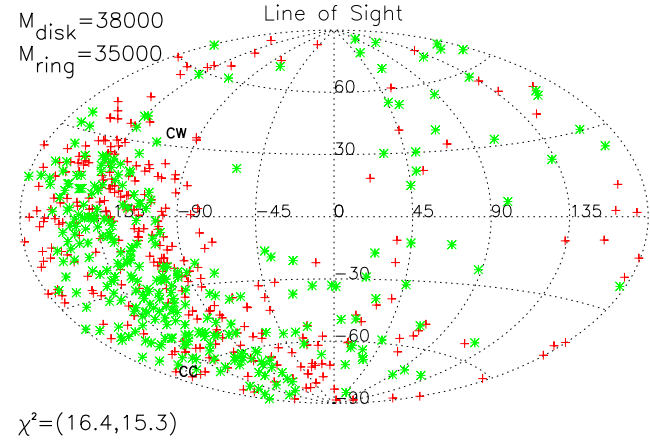


Figure 3. Same as Figures 1,2 but for the largest values of the disc and ring masses considered. The reduced χ^2 values for both the ring and the disc are much larger than the observed values. Such a stellar distribution cannot be classified as consisting of two discs at all.

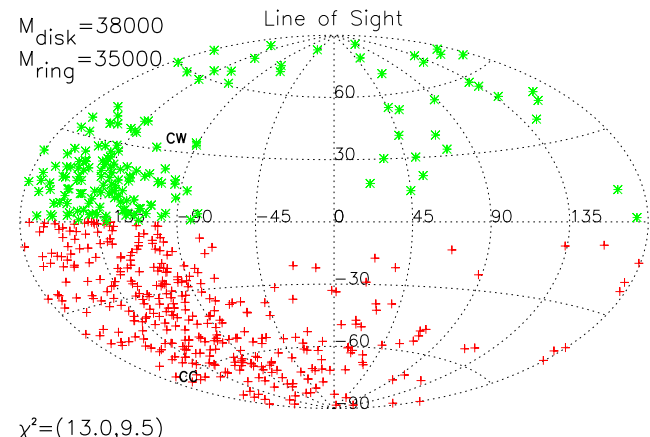


Figure 4. Same test as shown in Figure 3, but with stars divided into populations based on whether they rotate clock-wise or counter clock-wise ones. Note that the resulting χ^2 values are smaller but still much larger than the observed values.

them to the disc of their birth place. Certainly observationally such practice is impossible as it is not a priory known in which system the stars originated. Instead, one divides the stars on the clock-wise and the counter clock-wise ones (Genzel et al., 2003). To make a maximally fair comparison of the simulations with the data, at the end of the simulation, we assign particles to either the clock-wise or the counter clock-wise systems based on the sign of $J_z = (xv_y - yv_x)$, where x, y are the coordinates of the star. The resulting change is illustrated in Figure 4. The Figure demonstrates that when the stellar systems are warped to the degree that their orbits diffuse into one another's phase space, even a more careful division of orbits still fails to produce systems as well defined as those observed to exist near Sgr A*.

Table 1. Simulations results for circular initial orbits with the larger "ring", with $R = 5'' - 7''$. "fit quality" below, + or - sign, indicates whether the reduced χ^2 values are smaller or larger than the observed values. Clearly this is just a rough measure of the model's feasibility.

M_{disc}	M_{ring}	run	χ^2_{disc}	χ^2_{ring}	fit quality ^a
3500	1750	CL1	0.9	1.9	+
6300	1750	CL2	1.6	1.0	+
12000	1750	CL3	1.4	5.6	-
35000	1750	CL4	3.2	12.7	-
12000	3500	CL5	1.3	3.7	+
12000	10500	CL6	6.0	6.3	-
38000	10500	CL7	6.2	11.5	-
38000	35000	CL8	9.5	13.0	-

Table 2. Simulations results for circular initial orbits with the smaller ring, $R = 4'' - 5''$.

M_{disc}	M_{ring}	run	χ^2_{disc}	χ^2_{ring}	fit quality
3500	1750	CS1	0.9	1.5	+
6300	1750	CS2	1.2	1.0	+
12000	1750	CS3	1.	5.7	-
35000	1750	CS4	3.6	17.6	-
12000	3500	CS5	1.2	4.6	-
12000	10500	CS6	4.2	7.0	-
38000	10500	CS7	8.7	16.0	-
38000	35000	CS8	10.0	10.8	-

4 RESULTS

4.1 Circular initial orbits

Table 1 lists results of several runs with the larger stellar ring (i.e., $R = 5'' - 7''$). The first two column show the total stellar mass of the clock-wise (the disc) and the counter clock-wise (the ring) systems in Solar masses. The next column shows an identifier of the run (CL stands for "circular large"). Next two columns list the best fitting χ^2 values. The last column contains a "+" if the χ^2 values are smaller than the observed ones, and a "-" in the opposite case. Clearly this is not to be taken literally as in some cases the obtained χ^2 are just slightly larger than the observed ones.

In a similar fashion, the results of the tests with a smaller stellar ring (the counter clock-wise system, $R = 4'' - 5''$) are presented in Table 2. As one can see, the two tables are in general similar. The combined results of the small and larger scale ring tests are best described as these limits:

$$M_{\text{disc}} \lesssim 1.5 \times 10^4 M_{\odot} \quad (3)$$

$$M_{\text{ring}} \lesssim 1. \times 10^4 M_{\odot}. \quad (4)$$

4.2 Infalling star cluster: eccentric initial orbits

Levin et al. (2005) have recently modelled the dynamics of the stars peeled off from the IMBH inspiralling to smaller radii in the field of Sgr A*. The orbits of these stars were found to gain significant eccentricities due to repetitive in-

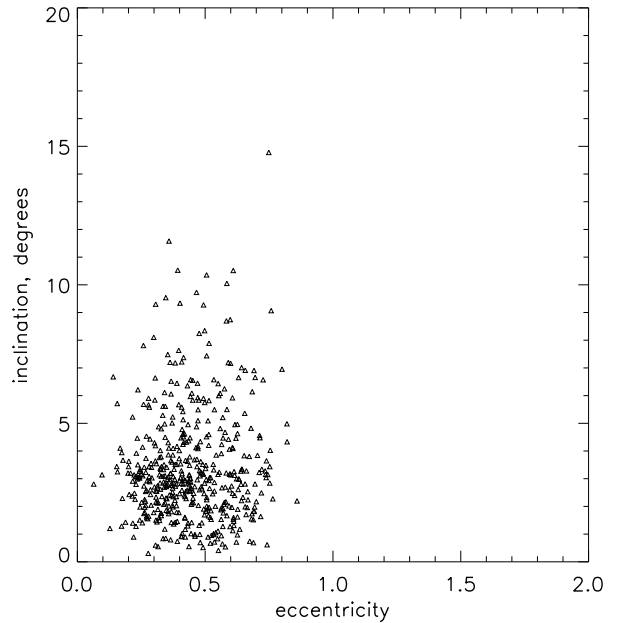


Figure 5. The initial distribution of eccentricities and inclination angles for a test with 500 particles in the clock-wise (disc) system. The distribution is chosen to mimic that resulting from a circular inspiral of an IMBH-star cluster (see Fig. 1 in Levin et al., 2005).

teractions with the IMBH while they have not yet distanced themselves very far from it. The effect is the strongest if the IMBH is itself on an eccentric orbit, when some of the stars are flung to orbits with an angular momentum opposing their initial one. Some of the stars in fact become unbound and escape to infinity. The eccentric star cluster inspiral thus defies the purpose of the model – to bring massive young stars in – as many are flung out on orbits in which they spend most of the time outside the central parsec. This would contradict observations (Genzel et al., 2003). We thus consider only the circular cluster inspiral model here. The stars then obtain (Levin et al., 2005) relatively mild eccentricities, with a median of around 0.5, and the resulting stellar disc is rather thin since the stellar velocities in the direction perpendicular to the IMBH inspiral orbit are quite small.

To generate initial orbits similar to those obtained by Levin et al. (2005), we place the stars radially in the same way as before, but we now add to their velocities random components both in the plane of the disc and perpendicular to the disc. In the plane of the disc, we added a random velocity component (in both radial and azimuthal directions), $\Delta\mathbf{v}$, distributed between $-(1/5)v_c$ to $+(1/5)v_c$, where v_c is the local circular speed. A smaller random component in the direction perpendicular to the disc was also given to imitate distribution of orbital inclinations to the system's plane. The resulting distribution of stellar initial eccentricities and inclinations (here defined with respect to their respective disc planes), shown in Figure 5, is indeed similar to Figure 1 of Levin et al. (2005).

The results of the tests with the given eccentricity and inclination distribution (Figure 5) are summarised in Table 3. The resulting χ^2 values are significantly larger than those

Table 3. Simulations results for eccentric initial orbits with larger ring.

M_{disc}	M_{ring}	run	χ^2_{disc}	χ^2_{ring}	fit quality
3500	1750	EL1	1.6	3.8	+
6300	1750	EL2	1.5	9.5	+
12000	1750	EL3	2.9	6.9	-
3500	3500	EL4	2.2	1.7	+
6300	3500	EL5	1.9	7.2	-
12000	3500	EL6	2.7	13.0	-
35000	3500	EL7	15.6	3.4	-
3500	10500	EL8	7.9	2.8	-
3500	14000	EL9	17.5	2.7	-
12000	10500	EL10	8.5	12.2	-
6650	10500	EL11	5.1	5.5	-
3500	7000	EL12	3.0	2.1	-

for the initially circular orbits at same masses. We estimate that the disc masses must be less than

$$M_{\text{disc}} \lesssim 5 \times 10^3 M_{\odot} \quad (5)$$

$$M_{\text{ring}} \lesssim 5 \times 10^3 M_{\odot}. \quad (6)$$

We interpret these tighter upper limits as a result of a wider spectrum of orbits in the eccentric discs. The greater diversity in the orbits leads to a greater difference in the rates at which the orbital planes precess.

4.3 The maximum current mass of the stellar systems

Using the same ideas described above, we can ask a slightly different question. We can start with orbits spread around in the velocity space sufficiently wide to yield χ^2 values consistent with the observed discs, follow these orbits for a shorter time, say a million year, and then measure the χ^2 again. If χ^2 significantly increases during this “short” time, such a disc should be rejected. The argument here is that during a time considerably shorter than the age of the discs, the observed system should not evolve (get warped and mixed) too much. We have ran a grid of models corresponding to disc and ring radii from the “larger” ring tests. The approximate upper limits on the masses of the system obtained in this way are

$$M_{\text{disc}} \lesssim 1 \times 10^4 M_{\odot} \quad (7)$$

$$M_{\text{ring}} \lesssim 5 \times 10^3 M_{\odot}. \quad (8)$$

5 DISCUSSION AND CONCLUSIONS

In this paper we modelled N-body evolution of two stellar discs guessing their initial geometrical arrangement based on their present day observed configuration, and then following stellar orbits for 3 Million years. Given the uncertainty in the initial guess, these tests cannot be precise, but since the discs are about twice older than 3 Million years (Paumard et al., 2005), we feel our upper mass limits are conservative. In summary, we found that the total mass of each of the stellar systems orbiting Sgr A* cannot be greater than $M \lesssim (5 - 15) \times 10^3 M_{\odot}$, with the lower values for eccentric

initial stellar orbits, and the higher limits for the circular orbits. It is somewhat disappointing to us that these limits are consistent with both of the models for star formation near Sgr A*. The minimum gaseous mass of the disc at which it becomes gravitationally unstable and forms stars is around $M_{\text{disc}} \simeq 10^4 M_{\odot}$ for Sgr A* case (Nayakshin & Cuadra, 2005). Note that this was derived from the basic Shakura & Sunyaev (1973) model, without including self-gravity into the hydrostatic balance equation for the disc. We expect the minimum M_{disc} to be another factor of ~ 2 lower, therefore. The mass of the stars formed through the disc collapse should be close to the original gas mass, as argued by Nayakshin & Cuadra (2005), because the viscous time scale for gas accretion is much longer than the time scale on which the stars can devour the disc. Thus the minimum stellar mass in that model is of order $5 \times 10^3 M_{\odot}$, in line with the upper limits obtained here.

Now, for the cluster infall model, the initial mass of the cluster should be as large as $10^5 - 10^6 M_{\odot}$ to allow it to spiral in rapidly enough, as well as to form an intermediate mass black hole that is heavy enough to prevent cluster dissolution away from the central parsec (Kim et al., 2004; Gürkan & Rasio, 2005). However the final stellar masses that make it into the central parsec are always a very small fraction of the original cluster mass, and they appear to be consistent with the limits obtained here.

We may also approach these mass limits from another angle. Estimating the total mass of the *observed* young massive stars, and assuming a standard Salpeter (1955) IMF, one would predict the total stellar mass to be around \sim (few to 10) $\times 10^4 M_{\odot}$, depending on the low mass cutoff in the power-law. This would be a factor of several larger than the mass limits for the circular initial orbits. Thus, if the stars were formed inside a massive self-gravitating disc, their IMF should be at least somewhat deficient in the low mass stars. In fact, in a separate paper, Nayakshin & Sunyaev (2005) show that a similar but even stronger argument can be made on purely observational grounds.

We thank an anonymous referee for his useful comments. This research was supported in part by the National Science Foundation under Grant No. PHY99-07949 during SN’s visit to the Kavli Institute for Theoretical Physics in Santa Barbara.

REFERENCES

Collin S., Zahn J., 1999, A&A, 344, 433
 Dehnen W., 2002, Journal of Computational Physics, 179, 27
 Eisenhauer F., Genzel R., Alexander T., et al., 2005, ApJ, 628, 246
 Genzel R., Schödel R., Ott T., et al., 2003, ApJ, 594, 812
 Gerhard O., 2001, ApJ, 546, L39
 Ghez A. M., Duchêne G., Matthews K., et al., 2003, ApJ, 586, L127
 Ghez A. M., Salim S., Hornstein S. D., et al., 2005, ApJ, 620, 744
 Goodman J., 2003, MNRAS, 339, 937
 Gürkan M. A., Rasio F. A., 2005, ApJ, 628, 236
 Kim S. S., Figer D. F., Morris M., 2004, ApJ, 607, L123
 Kim S. S., Morris M., 2003, ApJ, 597, 312
 Kolykhalov P. I., Sunyaev R. A., 1980, Soviet Astron. Lett., 6, 357
 Krabbe A., Genzel R., Eckart A., et al., 1995, ApJ, 447, L95
 Levin Y., Beloborodov A. M., 2003, ApJ, 590, L33

Levin Y., Wu A. S. P., Thommes E. W., 2005, ArXiv Astrophysics
e-prints

McMillan S. L. W., Portegies Zwart S. F., 2003, ApJ, 596, 314

Milosavljević M., Loeb A., 2004, ApJL, 604, L45

Nayakshin S., 2005, MNRAS, 359, 545

Nayakshin S., Cuadra J., 2005, A&A, 437, 437

Nayakshin S., Sunyaev R., 2005, MNRAS, 364, L23

Paczynski B., 1978, Acta Astron., 28, 91

Paumard T., Genzel R., Eisenhauer F., Ott T., Trippe S., 2005,
submitted to ApJ

Salpeter E. E., 1955, ApJ, 121, 161

Schödel R., Ott T., Genzel R., et al., 2002, Nature, 419, 694

Shakura N. I., Sunyaev R. A., 1973, A&A, 24, 337

Teuben P., 1995, in ASP Conf. Ser. 77: Astronomical Data Analysis Software and Systems IV, 398–+